

July 8, 2026

LaMET 2026 @ Jagiellonian University

Proton TMDPDFs from Lattice QCD

Spin Dependence of the Non-perturbative Transverse Structure

Jinchen He

In collaboration with ANL-BNL group



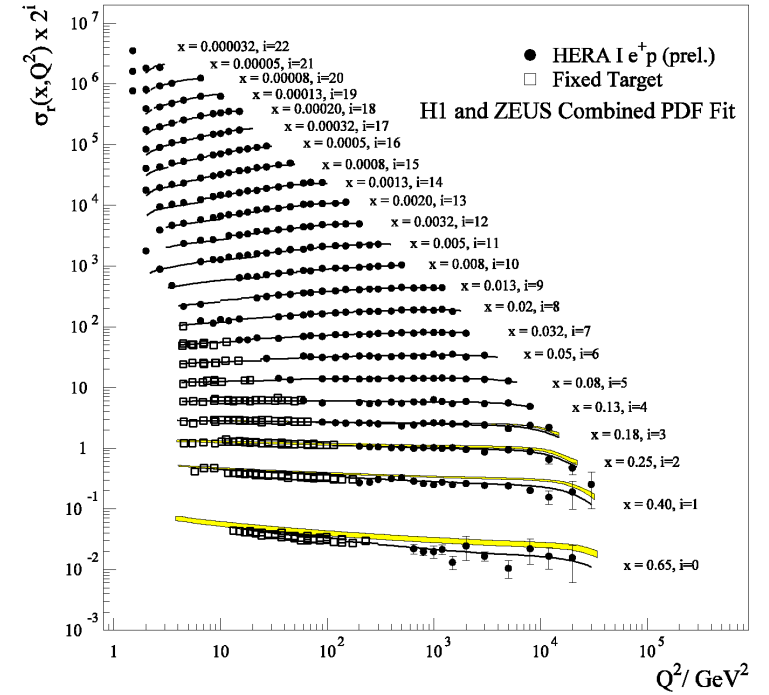
U.S. DEPARTMENT
of **ENERGY**

Fermi National Accelerator Laboratory is managed by
FermiForward for the U.S. Department of Energy Office of Science

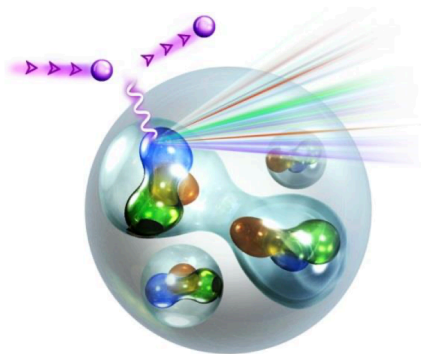
Parton Physics: Collinear structures

Bjorken scaling in 1968

- The structure functions are approximately independent of Q^2
- Evidence for point-like structures
- Parton model! *R. P. Feynman, Conf. Proc. C 690905 (1969)*
- Scaling violation at large $Q^2 \rightarrow$ running coupling in QCD



Collinear factorization in QCD



Cr. Dave Gaskell

$$\sigma_{\text{DIS}} \propto \left| \begin{array}{c} l \\ l' \\ q \\ P \end{array} \right|^2 \approx \left| \begin{array}{c} k \approx xP \\ p \\ P \end{array} \right|^2 \otimes \left| \begin{array}{c} l \\ l' \\ q \\ xP \end{array} \right|^2$$

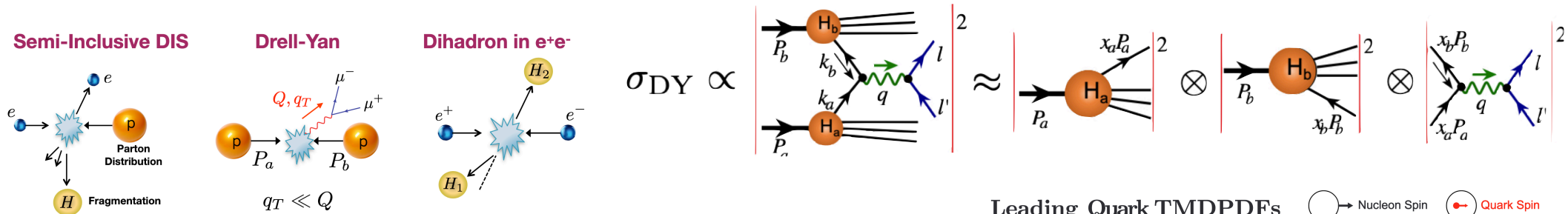
PDF Pert. Scattering

R. Boussarie, et al., "TMD Handbook", [arXiv:2304.03302 [hep-ph]]

Parton Physics: Collinear to TMD

TMD processes and TMD factorization

- TMD processes are important processes in high energy collisions, like Drell-Yan process on LHC and Semi-Inclusive DIS on EIC;



- But why we need TMD factorization? $\left\{ \begin{array}{l} \text{Scale separation} \\ \text{Large log: } \ln(Q/q_T) \\ \text{Soft mode} \end{array} \right.$

- When $q_T \sim Q$, collinear factorization is enough

$$\frac{d\sigma}{d^4q} = \sum_{i,j} \int_{x_a}^1 d\xi_a \int_{x_b}^1 d\xi_b \boxed{\text{PDF}} f_{i/H_a}(\xi_a) f_{j/H_b}(\xi_b) \frac{d\hat{\sigma}_{ij}(\xi_a, \xi_b)}{d^4q} \left[1 + O\left(\frac{\Lambda_{\text{QCD}}^2}{q_T^2}, \frac{\Lambda_{\text{QCD}}^2}{Q^2}\right) \right]$$

- When $\Lambda_{\text{QCD}} \lesssim q_T \ll Q$, TMD factorization is needed

$$\frac{d\sigma}{d^4q} = \frac{1}{s} \sum_{i \in \text{flavors}} \hat{\sigma}_i^{\text{TMD}}(Q) \int d^2\mathbf{k}_T \boxed{\text{TMD PDF}} f_{i/H_a}(x_a, \mathbf{k}_T) f_{i/H_b}(x_b, \mathbf{q}_T - \mathbf{k}_T) \left[1 + O\left(\frac{q_T^2}{Q^2}, \frac{\Lambda_{\text{QCD}}^2}{Q^2}\right) \right]$$

Leading Quark TMDPDFs \odot Nucleon Spin \odot Quark Spin

		Quark Polarization		
		Un-Polarized (U)	Longitudinally Polarized (L)	Transversely Polarized (T)
Nucleon Polarization	U	$f_1 = \odot$ Unpolarized		$h_1^\perp = \odot - \ominus$ Boer-Mulders
	L		$g_1 = \odot \rightarrow - \ominus \rightarrow$ Helicity	$h_{1L}^\perp = \odot \rightarrow - \ominus \rightarrow$ Worm-gear
	T	$f_{1T}^\perp = \odot - \ominus$ Sivers	$g_{1T}^\perp = \odot \rightarrow - \ominus \rightarrow$ Worm-gear	$h_1 = \uparrow \odot - \uparrow \ominus$ Transversity $h_{1T}^\perp = \uparrow \odot - \uparrow \ominus$ Pretzelosity

R. Boussarie, et al., 2304.03302 (2023)

Phenomenological Extractions of TMDs

Significant progress has been made in the phenomenological parameterizations of TMDs

- Collins-Soper kernel (CS kernel): rapidity evolution kernel of TMDs; Some of groups incorporate neural network;
A. Bacchetta, et al. (MAP) JHEP 08 (2024); V. Moos, et al., JHEP 11 (2025) ... Some of groups include lattice data;

- Pion TMDs

- Unpolarized *A. Vladimirov, JHEP 10 (2019); M. Cerutti, et al. (MAP), Phys.Rev.D 107 (2023); P. C. Barry, et al. (JAM) Phys.Rev.D 108 (2023)*

- Nucleon TMDs

- Unpolarized

M. Bury, et al., JHEP 10 (2022); A. Bacchetta, et al., JHEP 10 (2022); V. Moos, et al., JHEP 05 (2024); A. Bacchetta, et al., JHEP 08 (2024); V. Moos, et al., JHEP 11 (2025); P. Barry et al., 2510.13771 ...

- Helicity and Transversity

L. Gamberg, et al., PRD 106 (2022); A. Bacchetta, et al., PRL 134 (2025); ...

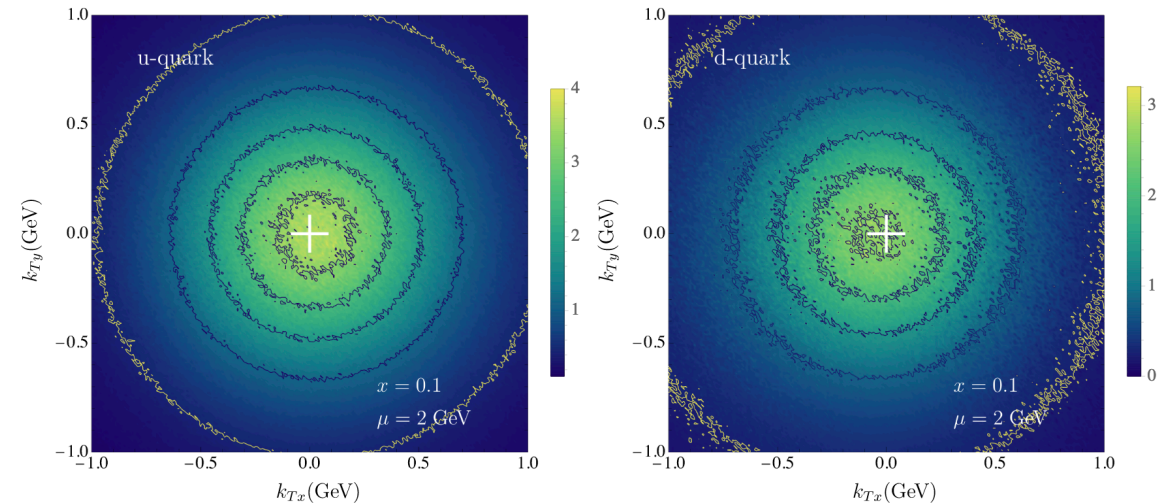
- Sivers

M. Bury, et al., PRL 126 (2021); I. P. Fernando, et al., Phys.Rev.D 108 (2023) ...

- Boer-Mulders

Z. Lu, et al., Phys.Rev.D 81 (2010); X. Liu, et al., Eur.Phys.J.C 81 (2021) ...

Tomographic scan of the nucleon via quark density function





Lattice Calculations of TMDs

Lattice QCD provides first-principles predictions of TMDs

- Mellin Moments; *B.U. Musch, et al., Phys.Rev.D 85 (2012); B. Yoon, et al., 1601.05717; B. Yoon, et al., Phys. Rev. D 96 (2017) ...*
- Large Momentum Effective Theory (LaMET)
 - CS kernel *M. H. Chu, et al. (LPC), JHEP 08 (2023); A. Avkhadiev et al., PRL 132 (2024); D. Bollweg, et al., Phys. Lett. B 852 (2024); J-X Tan, et al. (LPC), 2511.22547; A. Avkhadiev et al., 2510.26489, A. Francis et al., 2606.19221 ...*
 - Intrinsic soft functions *Q. A. Zhang, et al. (LPC), PRL 125 (2020); M. H. Chu, et al. (LPC), JHEP 08 (2023)*
 - Unpolarized TMD *JH, et al. (LPC), Phys.Rev.D 109 (2024); D. Bollweg, JH, et al., Phys.Rev.D 106 (2022);*
 - Helicity TMD *D. Bollweg, X. Gao, S. Mukherjee and Y. Zhao, PRL 135 (2025)*
 - Boer-Mulders TMD *L. Walter, et al. (LPC), PRD 111 (2025); L. Ma, et al. (LPC), JHEP 08 (2025)*

Large-Momentum Effective Theory (LaMET)

TMDPDF is defined from a light-cone correlator in a hadron, which is boost invariant.

$$f(x, b_{\perp}, \dots) = \int_{-\infty}^{\infty} \frac{db^{-}}{2\pi} e^{-ib^{-}(xP^{+})} \left\langle P \left| \bar{\psi}(b^{\mu}) W_{\square}(b^{\mu}, 0) \frac{\gamma^{+}}{2} \psi(0) \right| P \right\rangle \longleftrightarrow \left\langle |\vec{P}| = \infty \left| O(t=0) \right| |\vec{P}| = \infty \right\rangle$$

Define a quasi distribution with large-momentum states and time-independent operators.

$$\tilde{f}_{\Gamma}^0(x, b_{\perp}, P^z, \mu) = P^z \int \frac{dz}{2\pi} e^{iz(xP^z)} \frac{1}{2P^t} \langle P | \bar{\psi}_0(z, b_{\perp}) W_{\square}(z, b_{\perp}; 0) \Gamma \psi_0(0) | P \rangle$$



LaMET enables us to obtain the precision-controlled TMD PDFs in moderate x region.

$$\sqrt{S_I(b_{\perp}; \mu)} \cdot \tilde{f}_{\Gamma}(x, b_{\perp}, P^z; \mu) = f(x, b_{\perp}; \mu, \zeta) H_f(x, P^z; \mu) \exp \left[\frac{1}{2} \ln \frac{(2xP^z)^2}{\zeta} \gamma^{\overline{\text{MS}}}(b_{\perp}; \mu) \right] + \text{Power corrections}$$

Soft gluon radiation will lead to existence of soft functions

$$\sqrt{S_I(b_\perp; \mu)} \cdot \tilde{f}_\Gamma(x, b_\perp, P^z; \mu) = f(x, b_\perp; \mu, \zeta) H_f(x, P^z; \mu) \exp \left[\frac{1}{2} \ln \frac{(2xP^z)^2}{\zeta} \gamma^{\overline{\text{MS}}}(b_\perp; \mu) \right]$$

After regularization, the rapidity evolution is controlled by Collins-Soper scale: $\zeta = 2(xP^+)^2 e^{-2y_n}$

- Due to the factorization of the soft mode from the collinear mode, the soft function contains the well-

known rapidity divergence;

$$\underbrace{\int_{q_T}^Q \frac{dk}{k}}_{\text{full}} = \lim_{\tau \rightarrow 0} \left[\underbrace{\int_0^Q \frac{dk}{k} R_c(k, \tau)}_{\text{collinear}} + \underbrace{\int_{q_T}^\infty \frac{dk}{k} R_s(k, \tau)}_{\text{soft}} \right] = \ln \frac{Q}{q_T}$$

- The soft function can be separated into two parts:

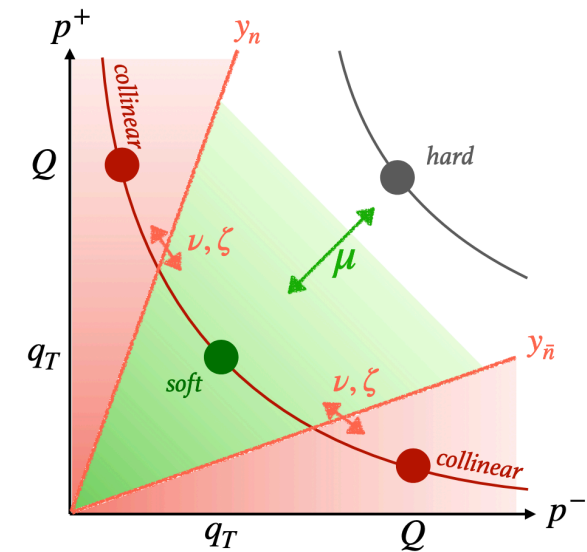
- Rapidity evolution kernel: CS kernel $\gamma^{\overline{\text{MS}}}(b_\perp; \mu)$

- Rapidity independent part: intrinsic soft function $\sqrt{S_I(b_\perp; \mu)}$

- CS kernel can be extracted from the rapidity evolution of TMDs

$$\tilde{\phi}_\Gamma(x, b_T, P_z; \mu) = A(x, b_T) H_\phi(x, \bar{x}, P_z; \mu) \exp \left[\ln \frac{P_z}{P_{\text{fix}}} \tilde{\gamma}(x, b_T) \right]$$

Here we do a fit on quasi-TMDWF at various pion momenta



R. Boussarie, et al., 2304.03302 (2023)

Extract intrinsic soft functions from large-momentum form factors

- The intrinsic soft function cannot be directly calculated on lattice because of two light-like

Wilson lines in different directions;

- Fortunately, it can be extracted from the meson form factor

$$F(b_{\perp}, P_1, P_2, \Gamma, \Gamma') \equiv -4N_c \frac{\langle P_2 | \bar{q}(b_{\perp}) \Gamma q(b_{\perp}) \bar{q}(0) \Gamma' q(0) | P_1 \rangle}{f_{\pi}^2(P_1 \cdot P_2)}$$

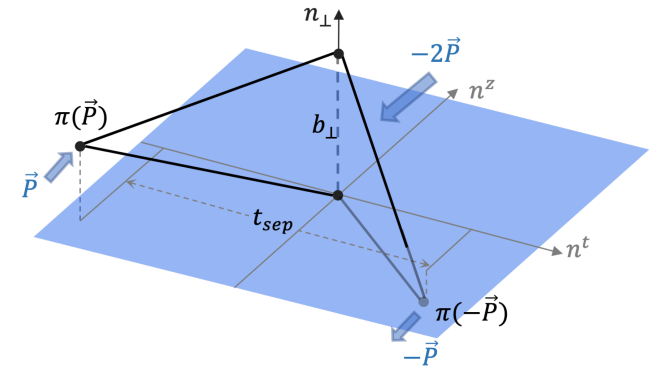
X. Ji, Y. Liu and Y. S. Liu, Nucl.Phys.B 955 (2020)

- The form factor satisfies the factorization formula

$$F(b_{\perp}, P^z) = \int dx_1 dx_2 H_F(x_1, x_2, P^z; \mu) \phi^{\dagger}(x_1, b_{\perp}, y_n; \mu, \zeta_1, \bar{\zeta}_1) \phi(x_2, b_{\perp}, -y_n; \mu, \zeta_2, \bar{\zeta}_2)$$

- Therefore, the intrinsic soft function can be extracted via

$$S_I(b_{\perp}; \mu) = \frac{F(b_{\perp}, P^z)}{\int dx_1 dx_2 H_F(x_1, x_2, P^z; \mu) \tilde{\Phi}^{\dagger}(x_1) \tilde{\Phi}(x_2)} \text{ where } \tilde{\Phi}(x) \equiv \frac{\tilde{\phi}_{\Gamma}(x, b_{\perp}, P^z; \mu)}{H_{\phi}(x, \bar{x}, P^z; \mu)}$$

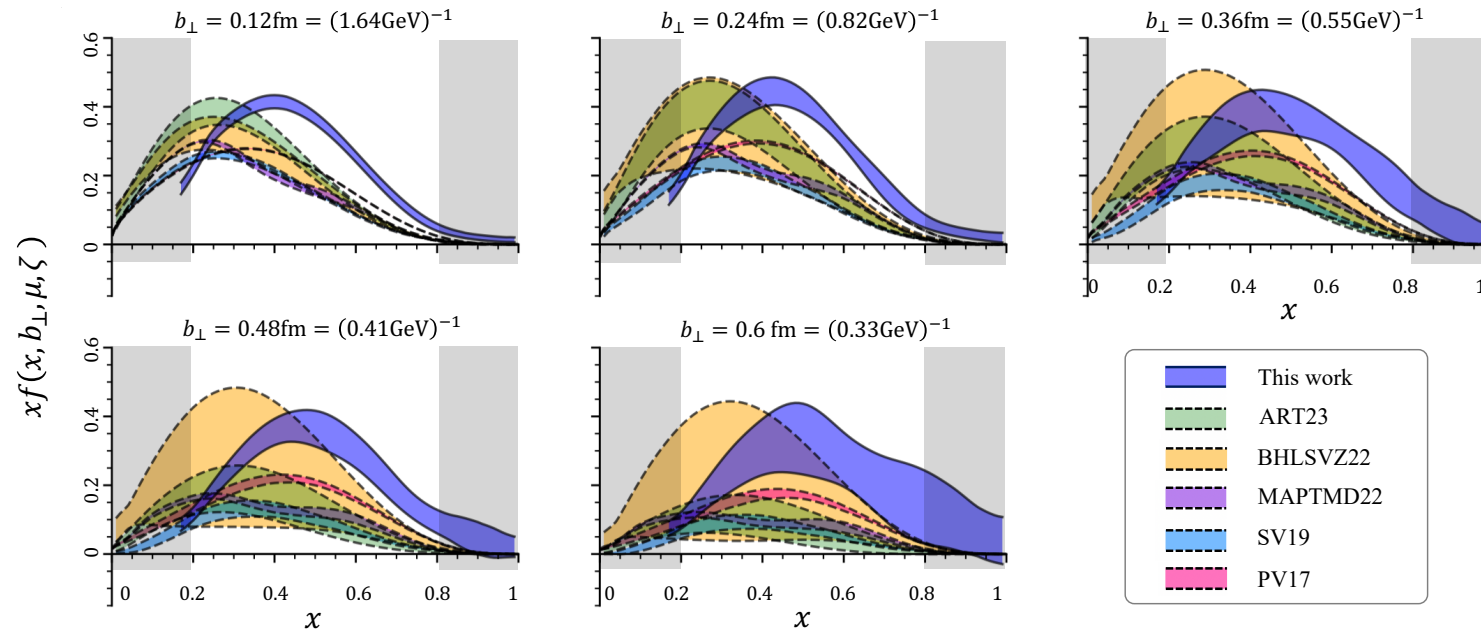


Q. A. Zhang, et al., Phys. Rev. Lett. 125 (2020)



Unpolarized Proton TMDPDFs

First lattice QCD calculation of x-dependent proton TMDPDFs



- ◆ $a = 0.12 \text{ fm}$
- ◆ $P_{\text{max}}^z = 2.58 \text{ GeV}$
- ◆ Physical limit of m_{π}^{val}
- ◆ N3LL matching
(Next-to-next-to-next-to-leading logarithmic)
- ◆ NLO soft function
(Next-to-leading order)

JH, et al. (LPC), Phys.Rev.D 109 (2024)

- Systematics are estimated and included in the final results;
- Constrained by the limited computing resources, it is hard to implement on a finer lattice;
- Due to the signal-to-noise ratio (SNR), it is hard to probe the large b_T region.

Now we have new techniques and more resources for better calculations, see Jin-Xin and Zhi-Chao's talks



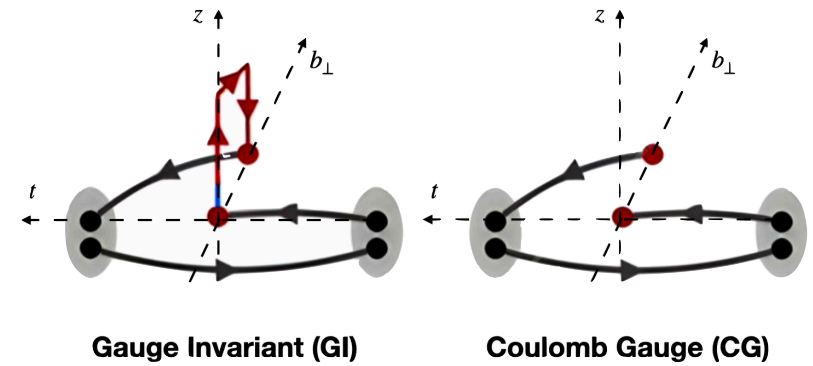
Coulomb Gauge Method

Define a quasi distribution in CG without Wilson line

$$\tilde{f}_{CG}^0(x, b_{\perp}, P^z, \mu) = P^z \int \frac{dz}{2\pi} e^{iz(xP^z)} \frac{1}{2P^t} \langle P | \bar{\psi}_0(z, b_{\perp}) \Gamma \psi_0(0) | \vec{\nabla} \cdot \vec{A} = 0 | P \rangle$$

Y. Zhao, PRL 133 (2024)

X. Gao, W. Y. Liu and Y. Zhao, PRD 109 (2024)



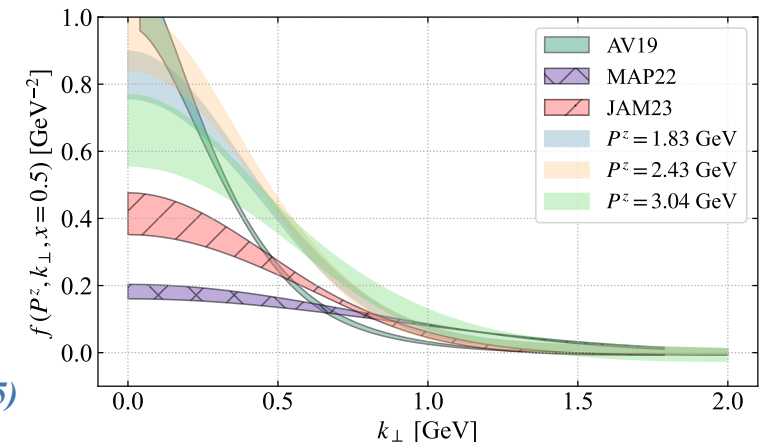
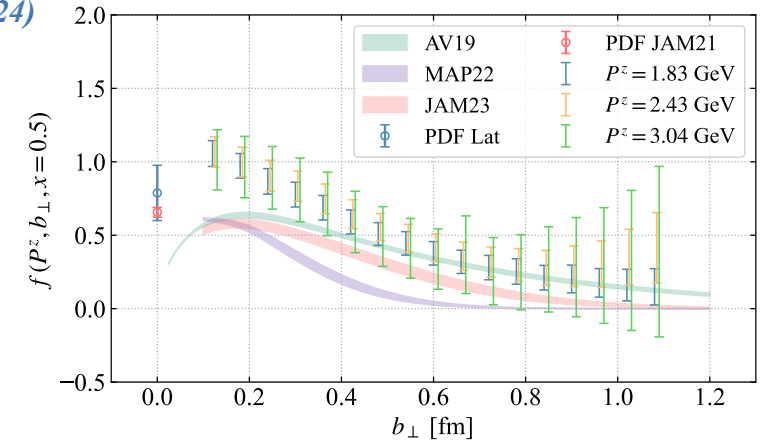
Why choose CG?

- The quasi distribution in CG belongs to the universality class in LaMET;
- No self-energy of the Wilson link, improving the SNR significantly;
- Simplified renormalization: $\bar{\psi}_0(z, b_{\perp}) \Gamma \psi_0(0) = Z_{\psi}(a) [\bar{\psi}(z, b_{\perp}) \Gamma \psi(0)]$;
- Larger off-axis momenta (3D rotational symmetry);
- A growing number of successful applications.

See also the talks by Qi, Bill, Yong and Xiang

D. Bollweg, X. Gao, JH, S. Mukherjee and Y. Zhao, PRD 112 (2025)

Pion unpolarized TMD PDFs





Lattice Setup

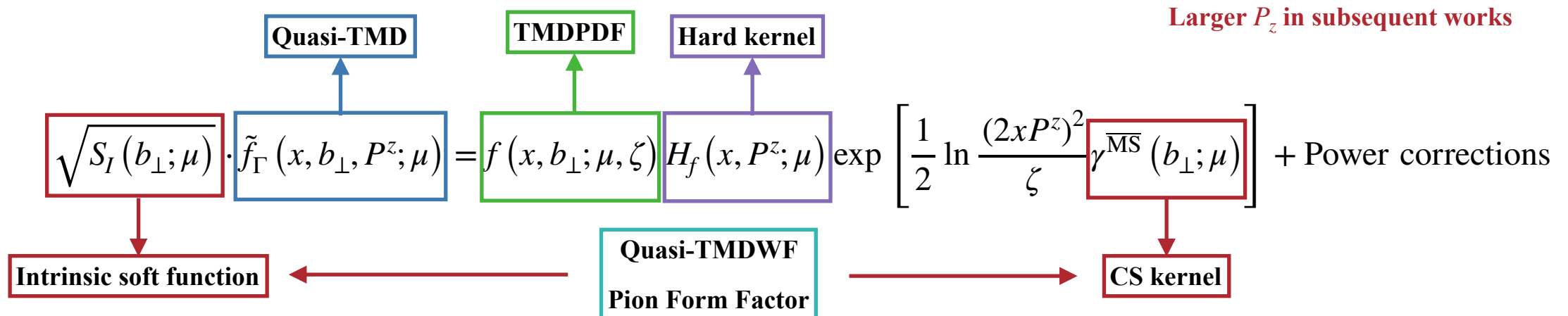
Extract intrinsic soft functions from large-momentum form factors

- 2+1-flavor **domain-wall** fermion (for both sea and valence quark) with Iwasaki gauge action;
 - **Physical pion mass** (for both sea and valence quark);
 - Lattice spacing is $a = 0.0836$ fm;
- Chiral fermion with strongly suppressed operator mixing**
*D. B. Kaplan, Phys.Lett.B 288 (1992);
T. Blum and Y. Shamir, 2603.27608*

- The proton quasi-TMD beam functions computed at proton momentum $P_z = 1.62$ GeV;

- The pion quasi-TMD wave functions with pion momenta up to $P_z = 1.85$ GeV;

- Pion form factors at momentum transfers up to $Q^2 = 13.7$ GeV².



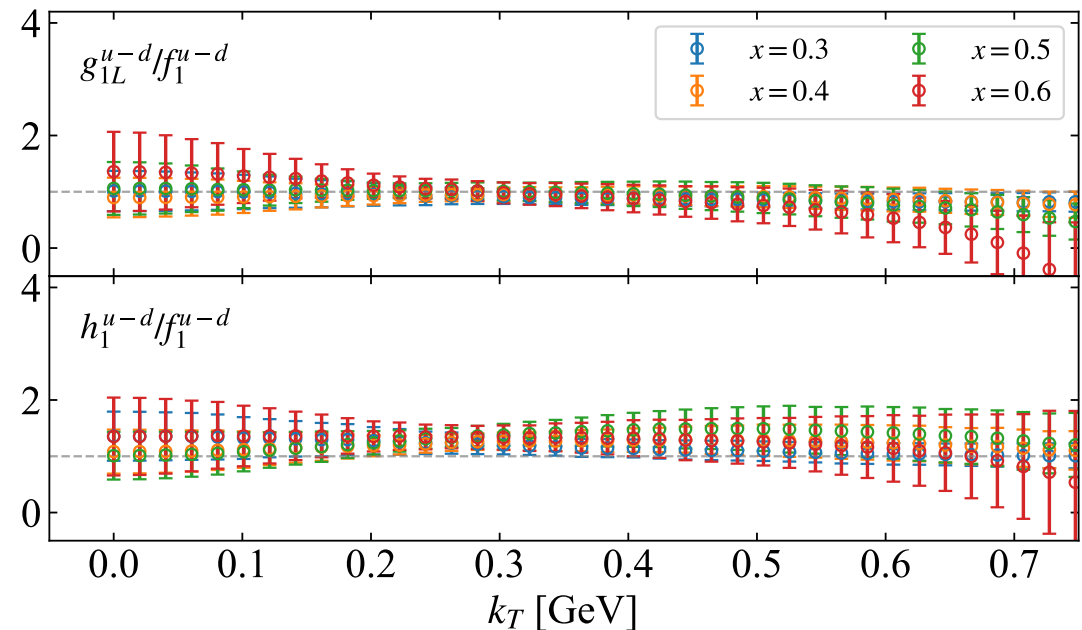
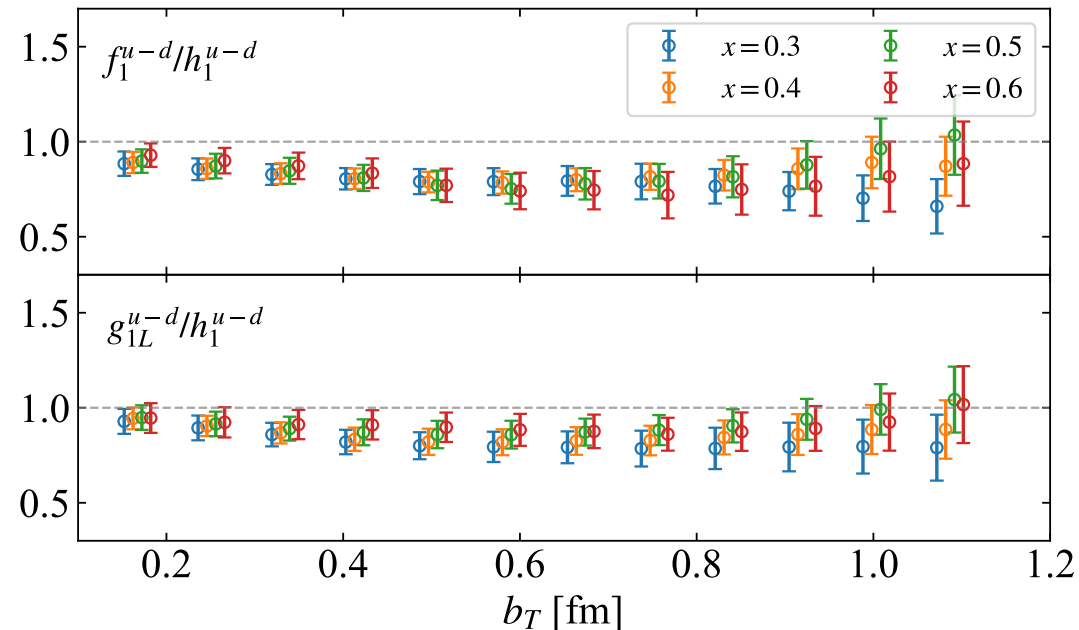


RGI Ratio of TMD PDFs

Ratio of TMD PDFs equals to the ratio of corresponding quasi-TMD beam functions

- This ratio is free from renormalization scheme and scale dependence;
- Thanks to the multiplicative matching, the ratio is independent from CS kernel, intrinsic soft functions;
- The non-perturbative transverse structure is largely insensitive to spin polarizations;
- The spin information primarily encoded in the longitudinal structure;

Consistent with the results in D. Bollweg et al., PRL 135 (2025)





Renormalization

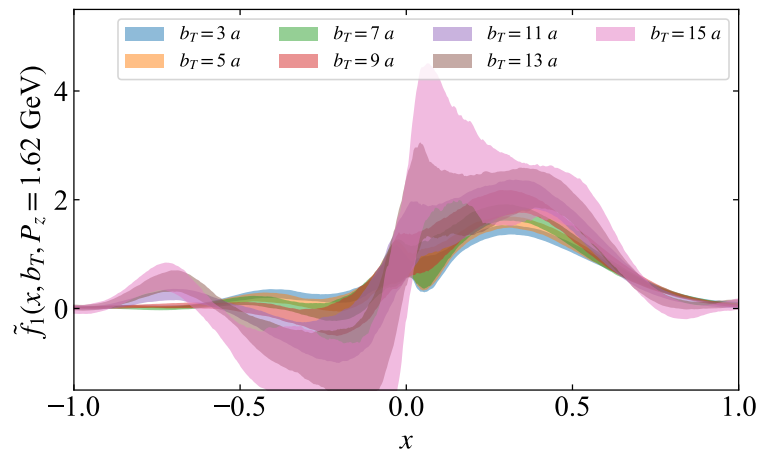
After renormalization, the universal large b_T behavior is mainly determined by the soft function

- The bare matrix elements of quasi-TMD beam functions and quasi-TMDWFs are renormalized as:

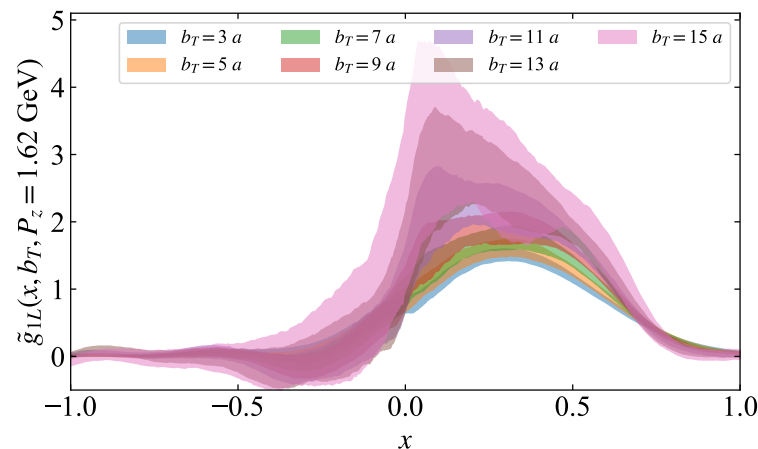
$$\tilde{h}_{\Gamma}(b_z, b_T, P_z; \mu) = \frac{\tilde{h}_{\Gamma}^0(b_z, b_T, P_z; a)}{\tilde{\varphi}_{\gamma^i \gamma^5}^0(0, b_T, 0; a)} \quad \text{and} \quad \tilde{\varphi}_{\Gamma}(b_z, b_T, P_z; \mu) = \frac{\tilde{\varphi}_{\Gamma}^0(b_z, b_T, P_z; a)}{\tilde{\varphi}_{\gamma^i \gamma^5}^0(0, b_T, 0; a)};$$

- In the moderate x region, quasi-TMD beam functions in all three polarizations show minor b_T -dependence;

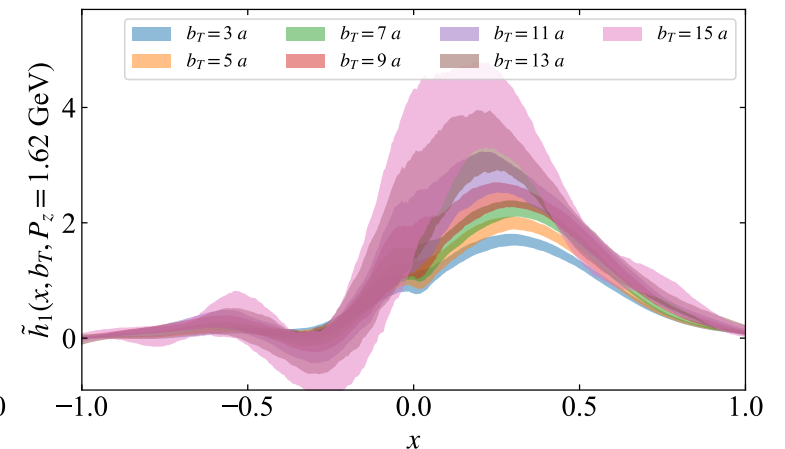
Unpolarized quasi-TMD



Helicity quasi-TMD



Transversity quasi-TMD



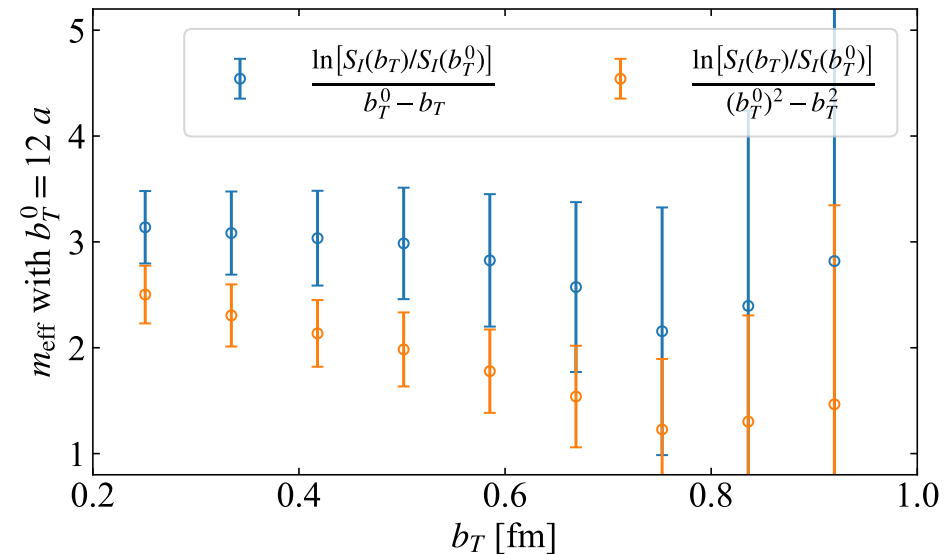
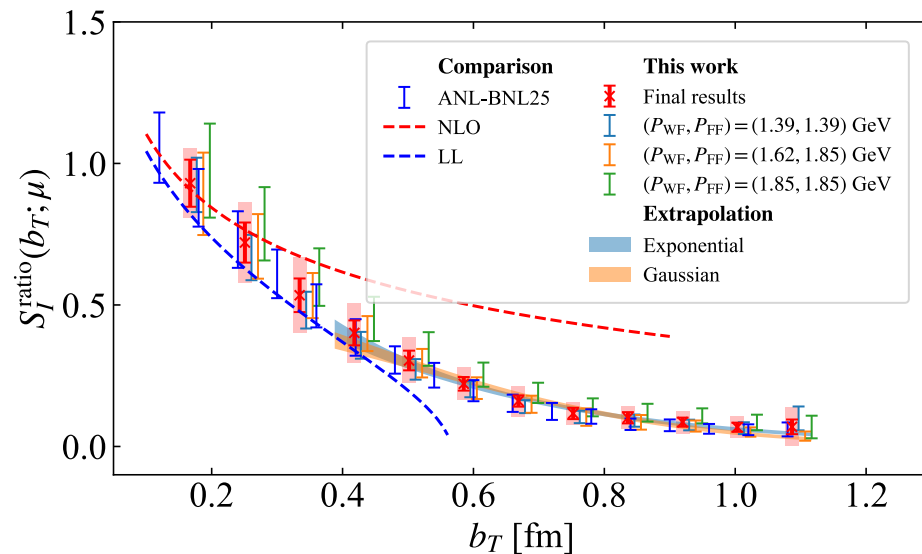


Intrinsic Soft Functions

Extract intrinsic soft functions at NLL from quasi-TMDWF and pion form factors

$$S_I(b_\perp; \mu) = \frac{F(b_\perp, P^z)}{\int dx_1 dx_2 H_F(x_1, x_2, P^z; \mu) \tilde{\Phi}^\dagger(x_1) \tilde{\Phi}(x_2)}$$

- Pion form factors at momentum transfers up to $Q^2 = 13.7 \text{ GeV}^2$;
- Large- b_T behavior: exponential (Ae^{-mb_T}) or gaussian ($Ae^{-m^2 b_T^2}$)?
- Fit results give $\chi^2/\text{d.o.f.} = 0.44$ v.s. 1.8 and $\log\text{GBF} = 19.54$ v.s. 13.02 (Bayes Factor of 680).



Effective mass plot also favors the exponential form

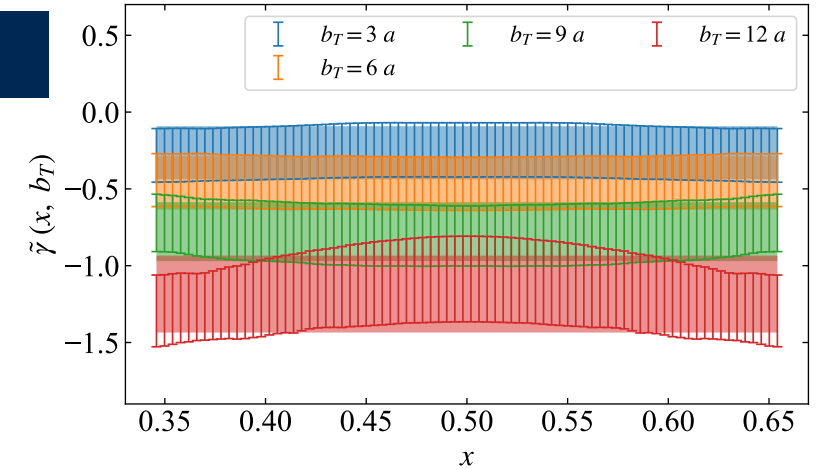


CS kernel

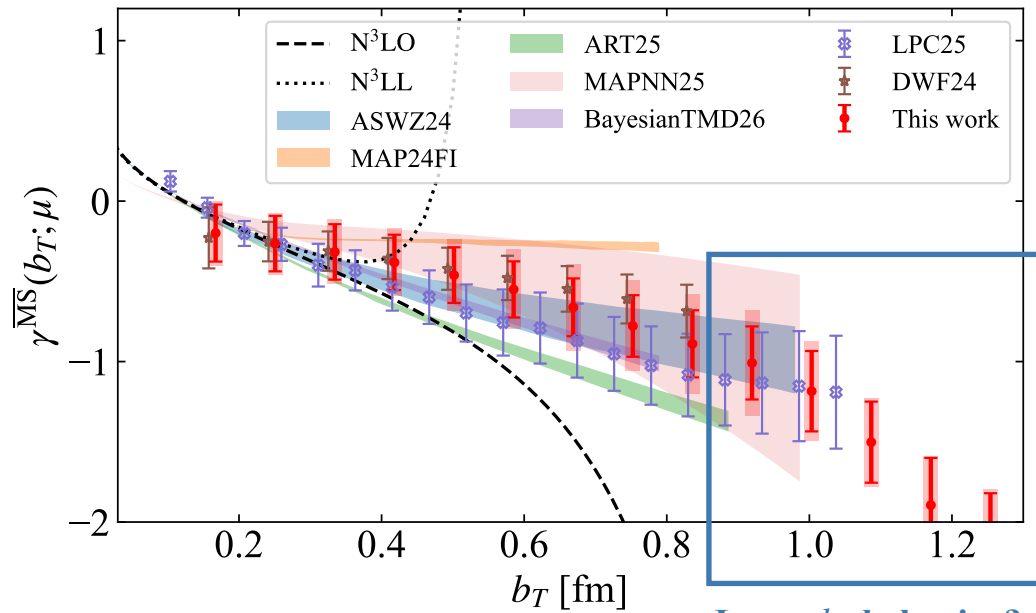
Extract CS kernel from quasi-TMDWF at different P_z

$$\tilde{\phi}_{\bar{\Gamma}}(x, b_T, P_z; \mu) = A(x, b_T) H_\phi(x, \bar{x}, P_z; \mu) \exp \left[\ln \frac{P_z}{P_{\text{fix}}} \tilde{\gamma}(x, b_T) \right]$$

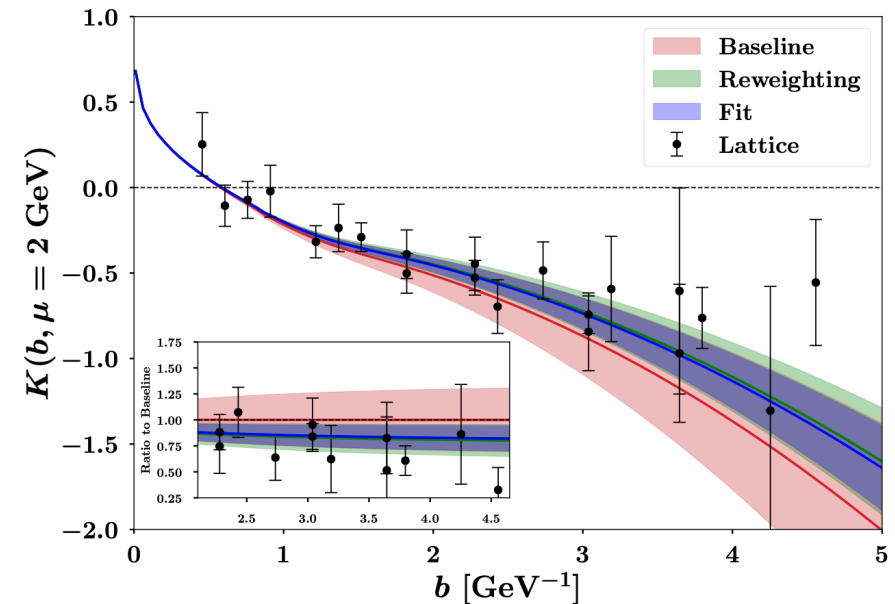
- Constant fits on $\tilde{\gamma}(x, b_T)$ for each b_T to get $\gamma^{\overline{\text{MS}}}$;
- Two sets of momenta are considered to estimate systematic error;



Good consistency with DWF24



Large b_T behavior?



A. Avkhadiev et al., Phys.Rev.Lett. 136 (2026)

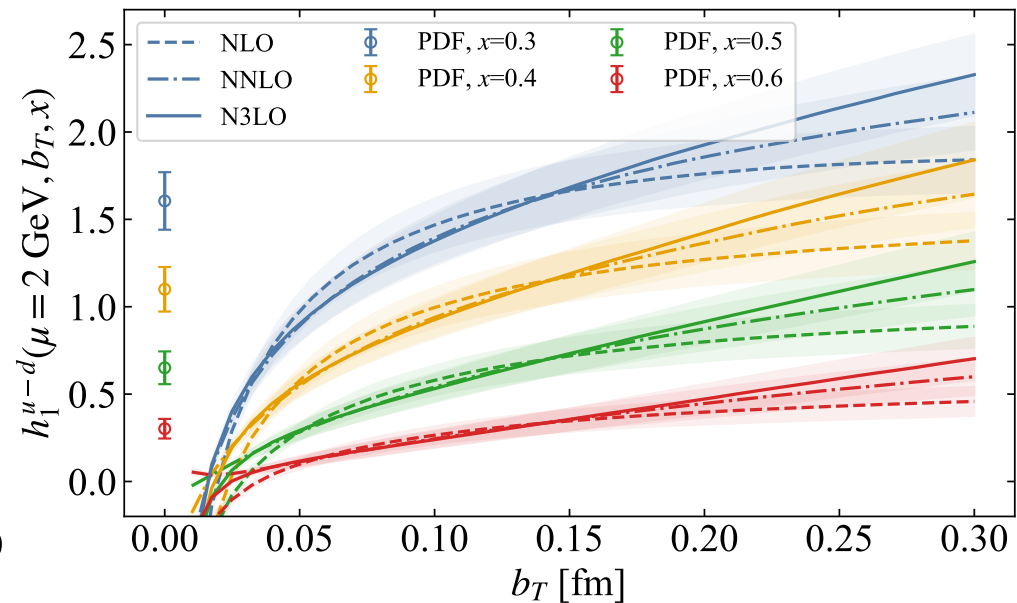
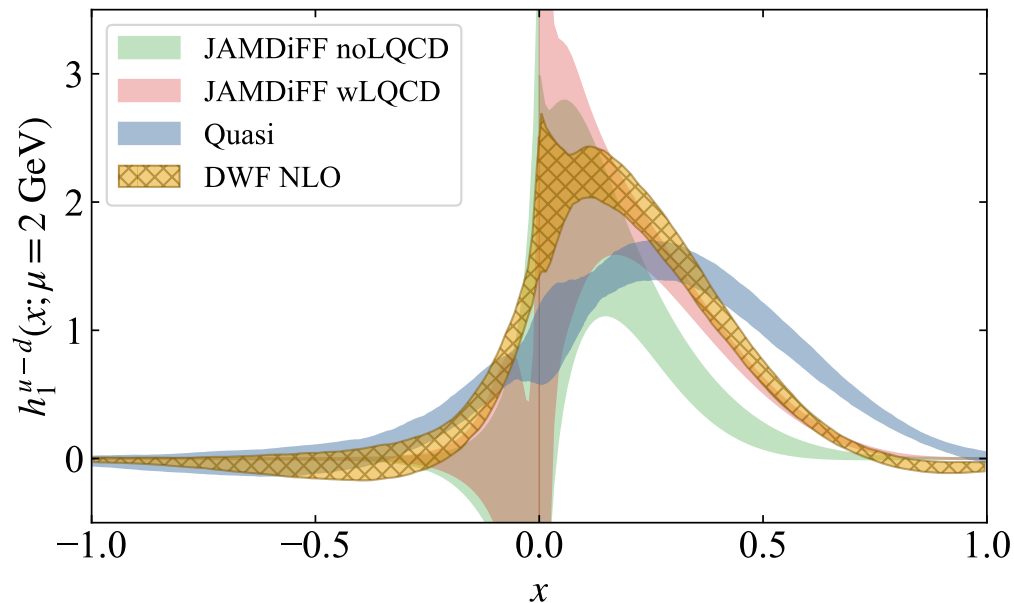


Short distance OPE

TMD PDFs admit an OPE onto the corresponding collinear PDFs at perturbative b_T

- The collinear PDFs can be extracted from correlators at $b_T = 0$, renormalized in hybrid scheme;
- OPE prediction is given as $f_{\Gamma}(x, b_T; \mu, \zeta) = C_{\Gamma}(x, b_T; \mu, \zeta) \otimes f_{\Gamma}^{\text{coll}}(x, \mu) + \mathcal{O}(b_T^2 \Lambda_{\text{QCD}}^2)$;
- The short distance matching kernels are available up to N3LO, showing a good convergence;

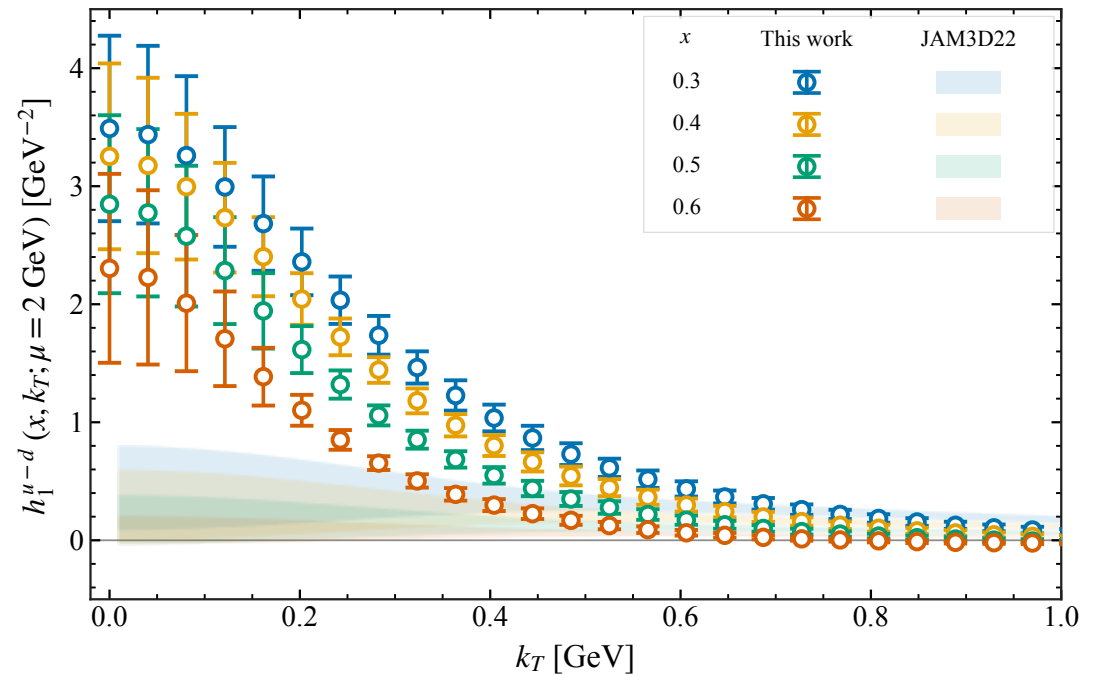
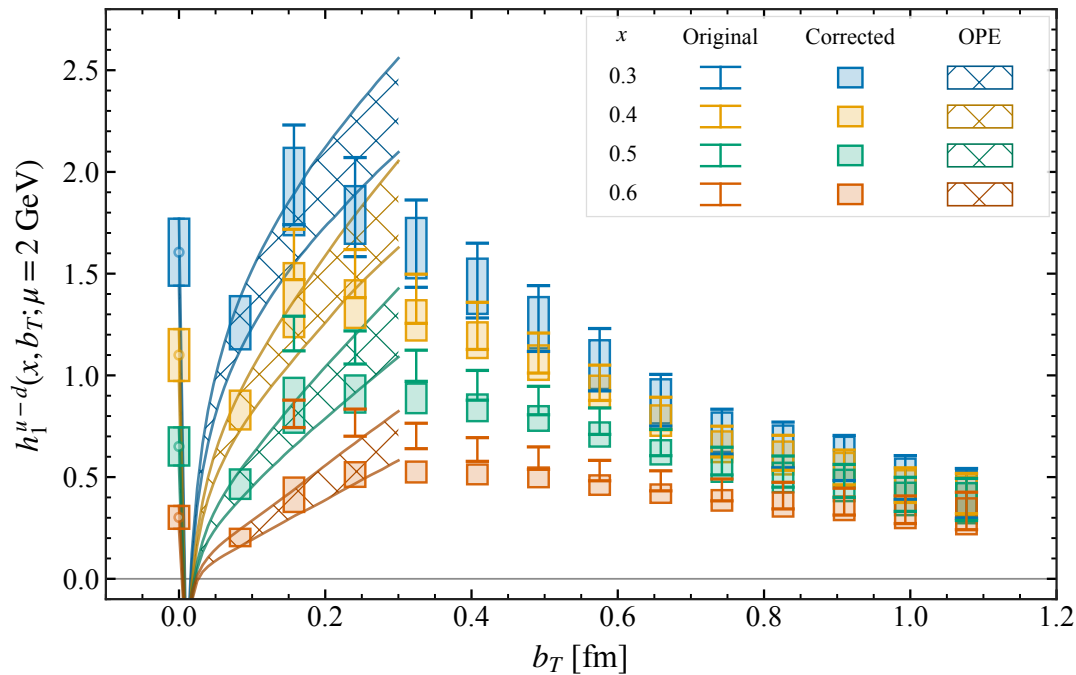
M.-X. Luo et al., JHEP 06 (2021) 115; Y. Zhu, JHEP 02 (2026) 115; Y. Zhu, JHEP 03 (2026)



Transversity TMD PDFs

TMD PDFs in transverse coordinate and momentum space

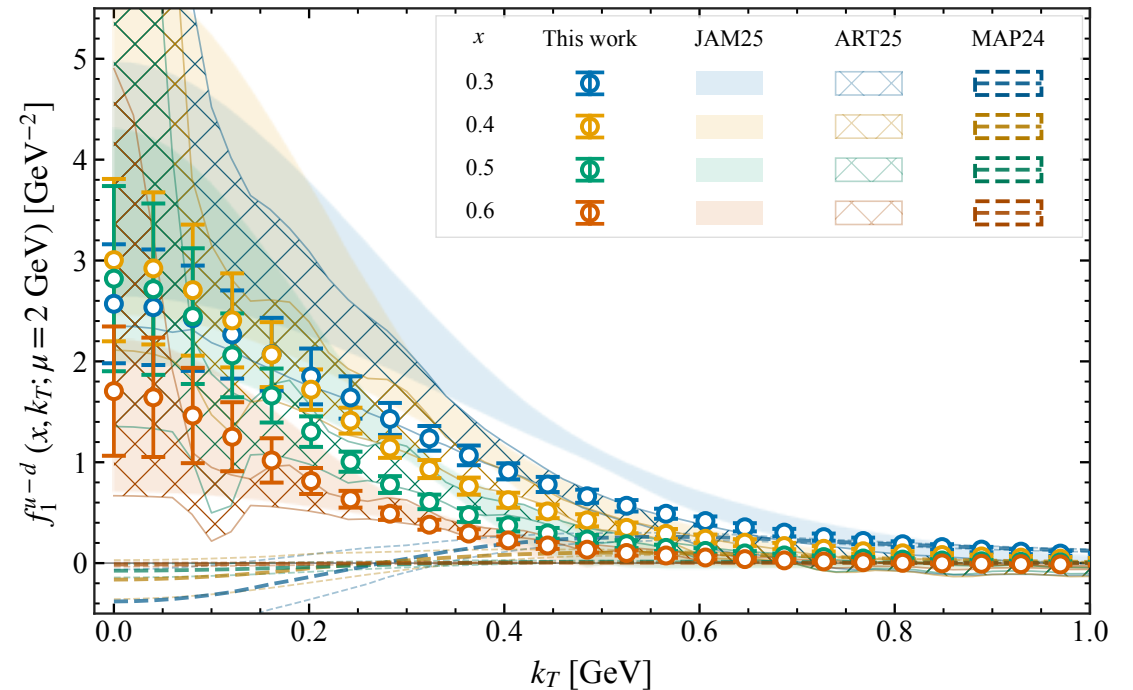
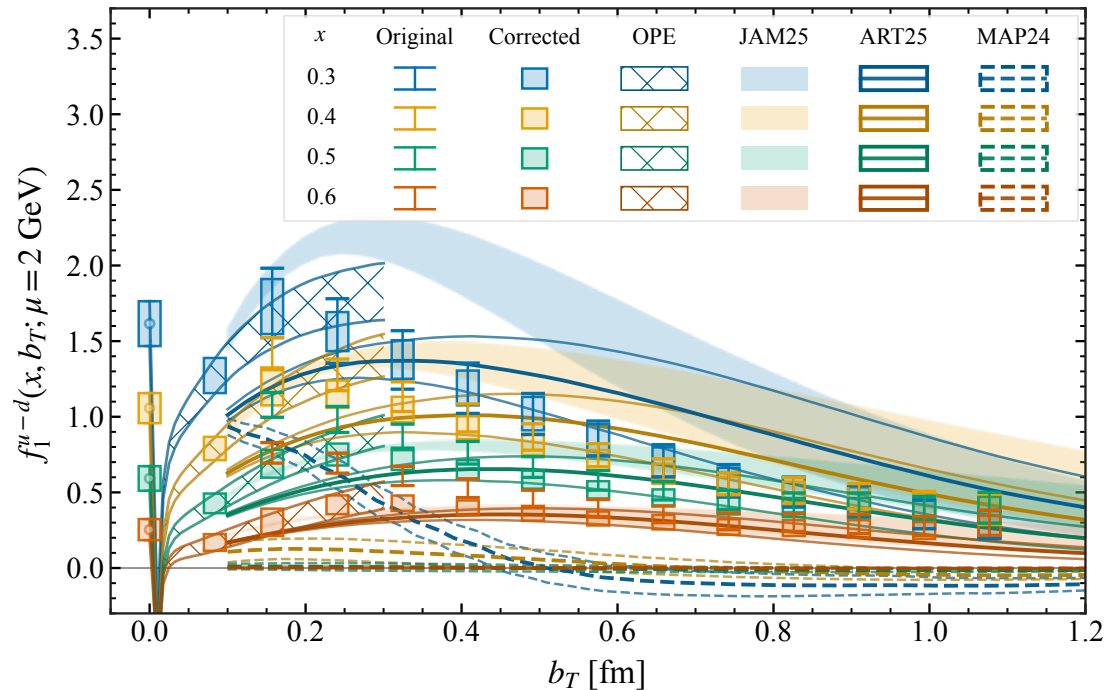
- The short b_T region is corrected by a $\delta C(x, b_T, P_z) = 1 + c/(2xb_T P_z)$ to match OPE results;
- The large b_T region is extrapolated using exponential form (Ae^{-mb_T}) with loose prior from soft functions;



Unpolarized TMD PDFs

TMD PDFs in transverse coordinate and momentum space

- The short b_T region is corrected by a $\delta C(x, b_T, P_z) = 1 + c/(2xb_T P_z)$ to match OPE results;
- The large b_T region is extrapolated using exponential form (Ae^{-mb_T}) with loose prior from soft functions;

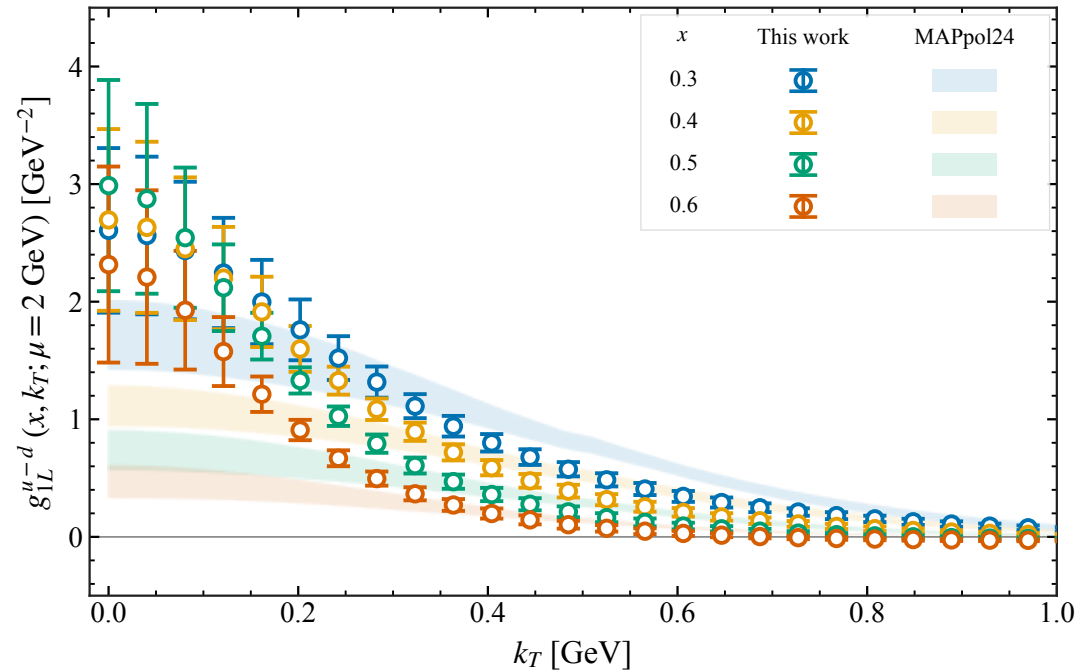
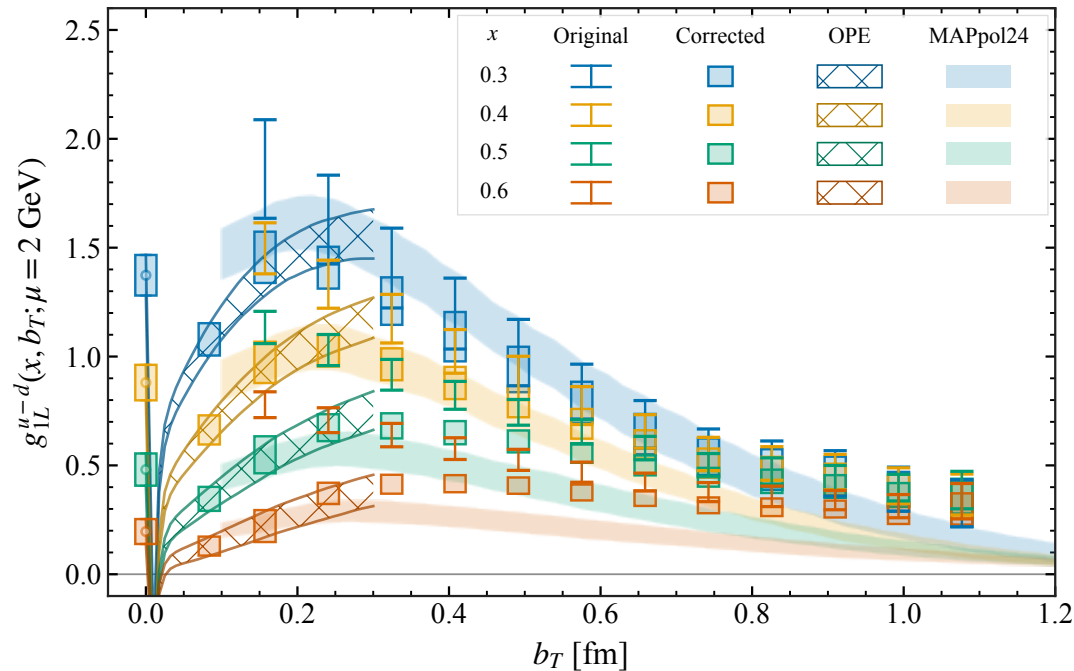




Helicity TMD PDFs

TMD PDFs in transverse coordinate and momentum space

- The short b_T region is corrected by a $\delta C(x, b_T, P_z) = 1 + c/(2xb_T P_z)$ to match OPE results;
- The large b_T region is extrapolated using exponential form (Ae^{-mb_T}) with loose prior from soft functions;





Conclusion

Proton TMDPDFs from Lattice QCD

- We have presented the **first simultaneous** lattice-QCD determination of full isovector **proton** light-cone TMDPDFs in the **unpolarized, helicity, and transversity** channels;
- Although the three channels have distinct spin structures and different normalizations, their **non-perturbative transverse structures** are similar within the current uncertainties;
- After renormalization, the large- b_T behavior of TMD PDFs is dominated by the **intrinsic soft function**;
- After combining the **short distance OPE** and large distance extrapolation, the k_T -space TMDPDFs provides a spin-dependent three-dimensional proton tomography;
- In future work, we will generalize to **larger P_z and multi-ensemble analysis**.



LaMET-Agent: For Data Analysis in LaMET

Why we need LaMET-Agent?

- **Recent advances in precision control** have increased the **implementation complexity** of LaMET. As a result, adopting LaMET formalism often requires either **close collaboration with LaMET experts** or a **substantial investment of time** to handle the technical details. LaMET Agent lowers this implementation barrier, making the formalism more accessible to a **broader community**;
- **For researchers new to LaMET**: the agent makes LaMET data analysis accessible and helps users understand the **correct** analysis workflow and methodology;
- **For experienced LaMET users**: the agent automates routine analysis tasks, accelerates the workflow, and allowing researchers to focus on physics instead of implementation;
- LaMET-Agent provides a standard, well-organized, understandable workflow.

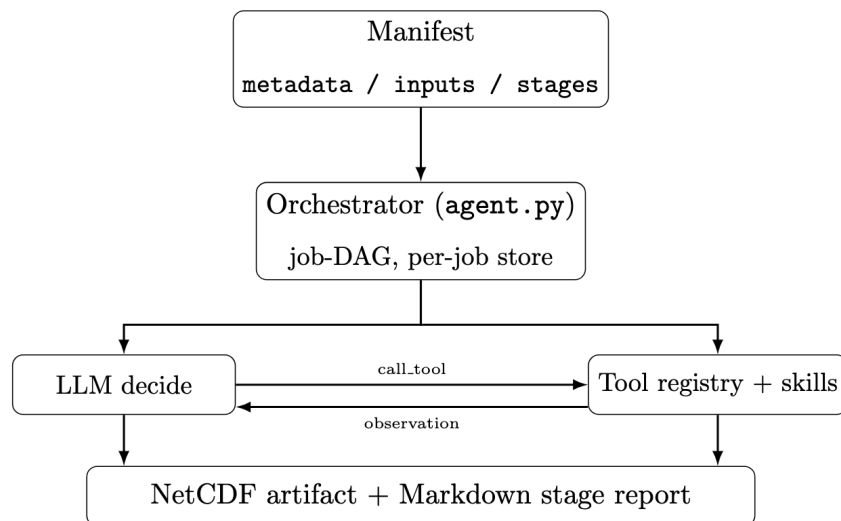
In collaboration with Xiangyu Jiang, Fei Yao and Dian-Jun Zhao



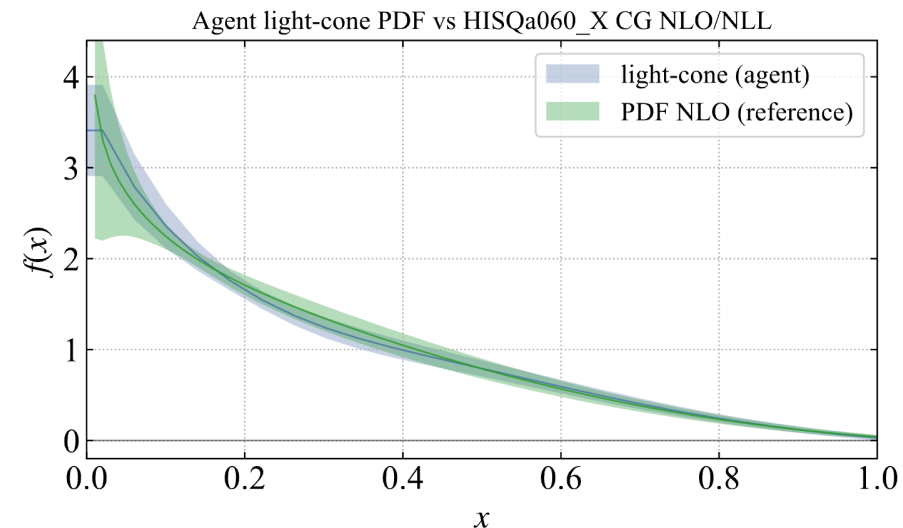
LaMET-Agent: For Data Analysis in LaMET

A delicate combination of deterministic pipelines and LLM decisions

- Six stages: Correlator Analysis, Renormalization, Fourier Transform, Perturbative Matching, Physical Extrapolation, Review;
- Single-run workflow for multi-ensemble analyses; unified NetCDF-based data management; stage reports for transparency; easily extensible to new observables and analysis techniques.



Reproducing the Pion PDF with LaMET Agent



X. Gao, W. Y. Liu and Y. Zhao, PRD 109 (2024)



Thank you!

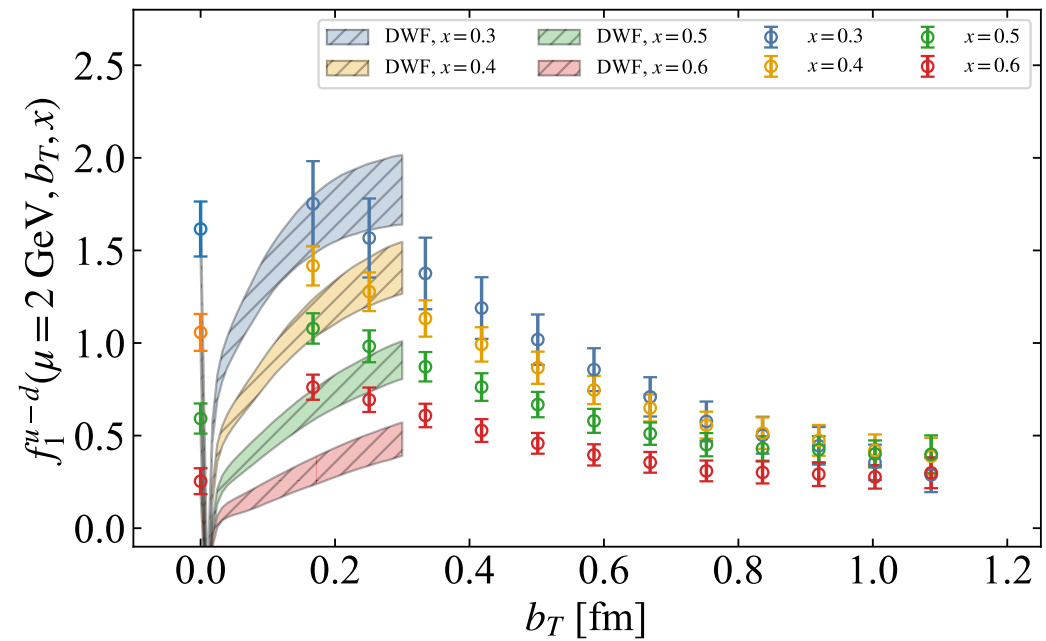
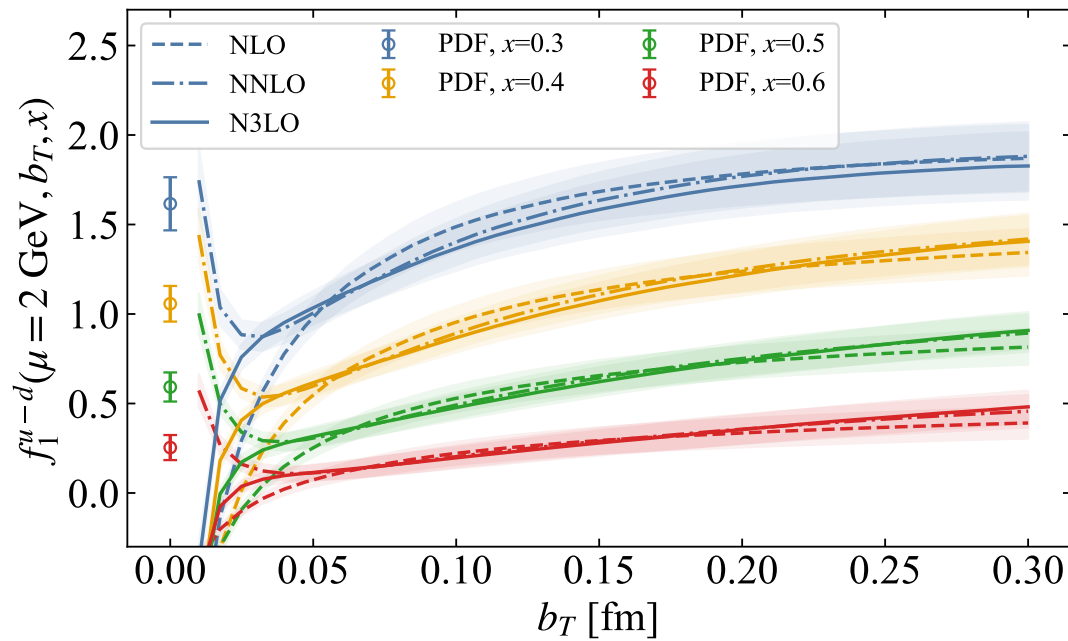
Jinchen He @ LaMET 2026



Short distance OPE

TMD PDFs admit an OPE onto the corresponding collinear PDFs at perturbative b_T

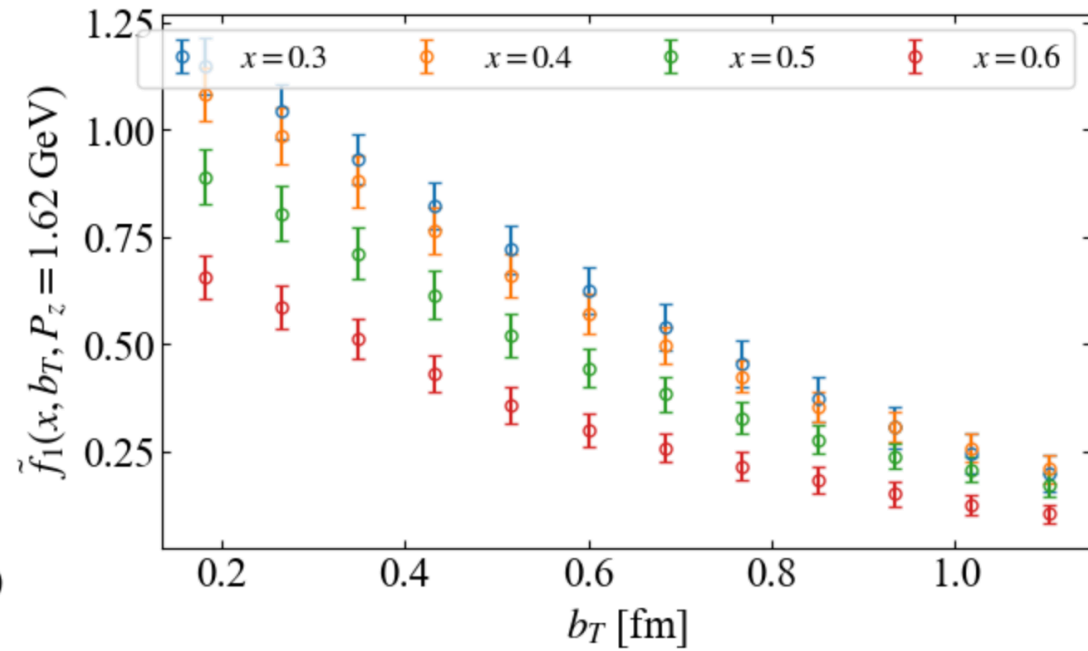
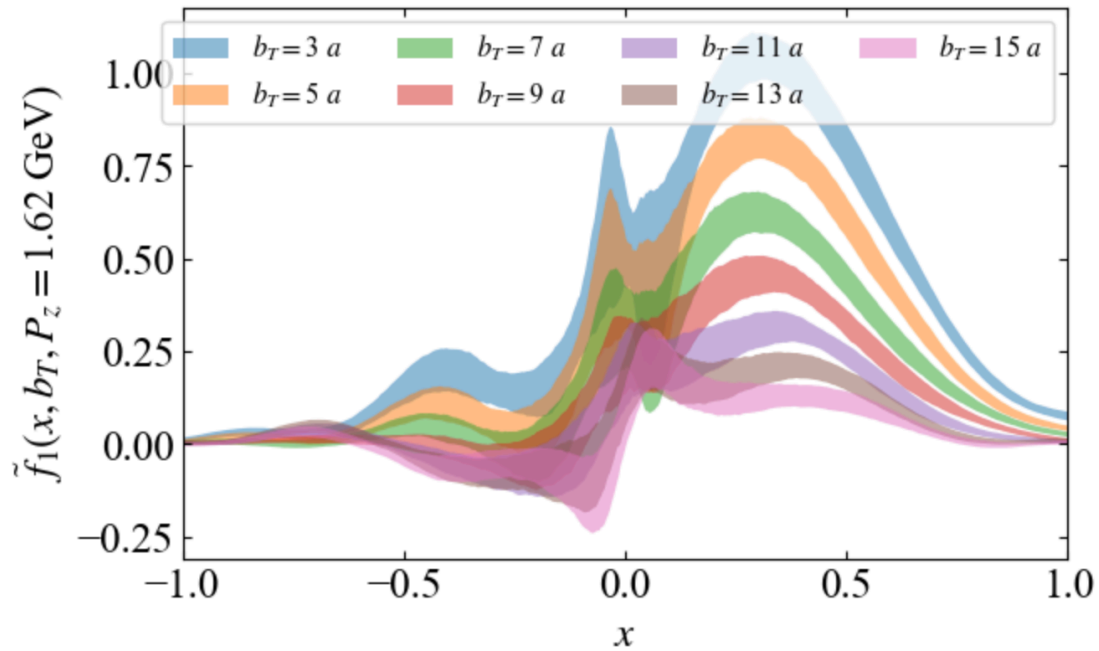
- The intrinsic soft function cannot be directly calculated on lattice because of two light-like
- $f_{\Gamma}^{\mu-d}(x, b_T; \mu, \zeta) = C_{\Gamma}(x, b_T; \mu, \zeta) \otimes f_{\Gamma}^{\text{coll}}(x, \mu) + \mathcal{O}(b_T^2 \Lambda_{\text{QCD}}^2)$





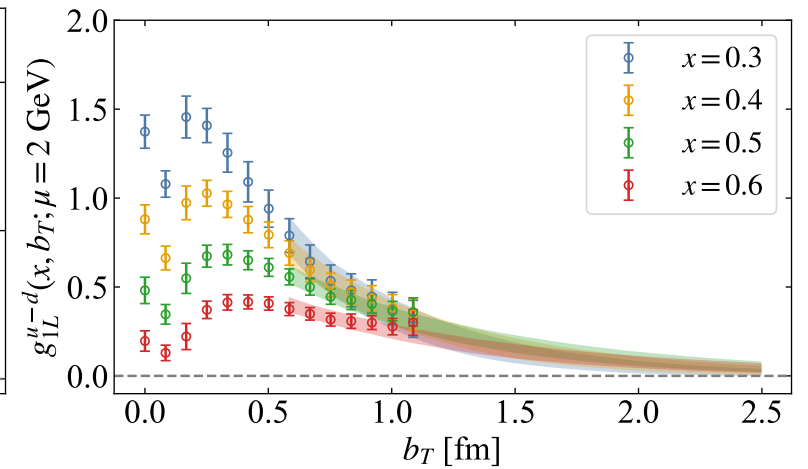
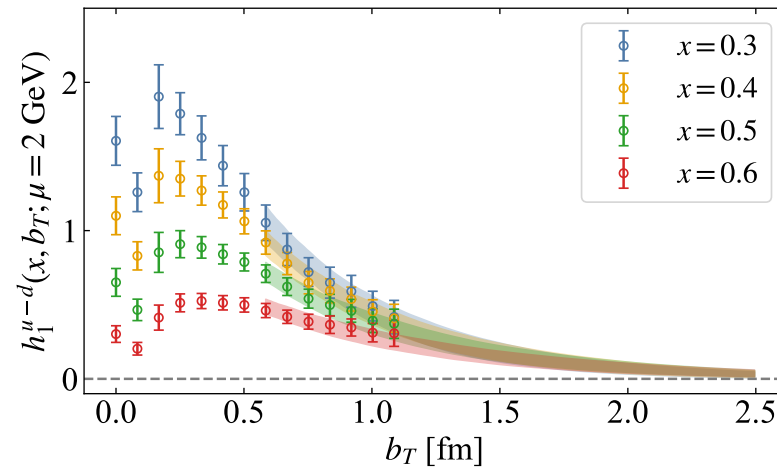
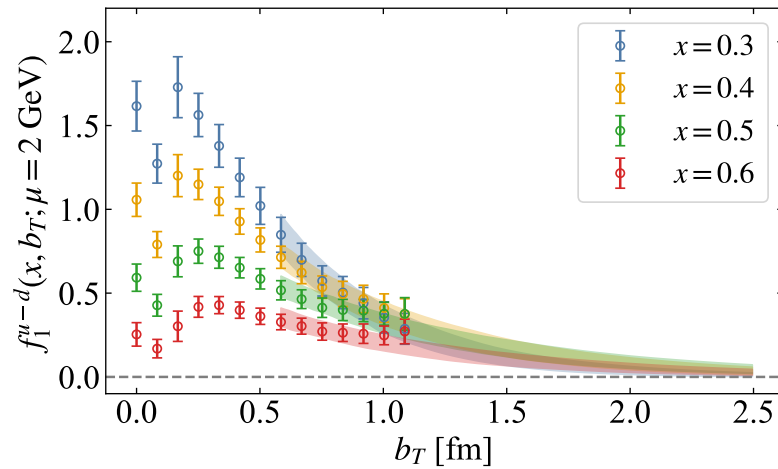
bT Dependence of Bare qTMD

What if before renormalization?



✚ Extrapolation in Larger bT Region

Extrapolation using the exponential form and loose prior from soft functions



Soft Functions in TMD Factorization

$$\frac{d\sigma}{dQdYd^2\mathbf{q}_T} = \left(\frac{d\sigma^W}{dQdYd^2\mathbf{q}_T} + \frac{d\sigma^Y}{dQdYd^2\mathbf{q}_T} \right) \left[1 + \mathcal{O}\left(\frac{\Lambda_{\text{QCD}}^2}{Q^2}\right) \right].$$

$$\frac{d\sigma^W}{dQdYd^2\mathbf{q}_T} = \sum_{\text{flavors } i} H_{i\bar{i}}(Q^2, \mu) \int d^2\mathbf{b}_T e^{i\mathbf{b}_T \cdot \mathbf{q}_T} \tilde{f}_{i/p}(x_a, \mathbf{b}_T, \mu, \zeta_a) \tilde{f}_{\bar{i}/p}(x_b, \mathbf{b}_T, \mu, \zeta_b) \quad (2.29a)$$

$$= \sum_{\text{flavors } i} H_{i\bar{i}}(Q^2, \mu) \int d^2\mathbf{b}_T e^{i\mathbf{b}_T \cdot \mathbf{q}_T} \tilde{B}_{i/p}(x_a, \mathbf{b}_T, \mu, \zeta_a/v^2) \tilde{B}_{\bar{i}/p}(x_b, \mathbf{b}_T, \mu, \zeta_b/v^2) \times \tilde{S}_{n_a n_b}(b_T, \mu, \nu). \quad (2.29b)$$

$$\tilde{f}_{i/p}(x, \mathbf{b}_T, \mu, \zeta) = \tilde{B}_{i/p}(x, \mathbf{b}_T, \mu, \zeta/v^2) \sqrt{\tilde{S}_{n_a n_b}(b_T, \mu, \nu)}, \quad (2.32)$$

$$\begin{aligned} \tilde{B}_{i/p}(x, \mathbf{b}_T, \mu, \zeta/v^2) &= \lim_{\substack{\epsilon \rightarrow 0 \\ \tau \rightarrow 0}} \tilde{Z}_B^i(b_T, \mu, \nu, \epsilon, \tau, xP^+) \tilde{B}_{i/p}^0(x, \mathbf{b}_T, \epsilon, \tau, xP^+) \\ &= \lim_{\substack{\epsilon \rightarrow 0 \\ \tau \rightarrow 0}} \tilde{Z}_B^i(b_T, \mu, \nu, \epsilon, \tau, xP^+) \frac{\tilde{f}_{i/p}^{0(u)}(x, \mathbf{b}_T, \epsilon, \tau, xP^+)}{\tilde{S}_{n_a n_b}^{0\text{subt}}(b_T, \epsilon, \tau)}, \end{aligned} \quad (2.34)$$

$$\tilde{S}_{n_a n_b}(b_T, \mu, \nu) = \lim_{\substack{\epsilon \rightarrow 0 \\ \tau \rightarrow 0}} \tilde{Z}_S(b_T, \mu, \nu, \epsilon, \tau) \tilde{S}_{n_a n_b}^0(b_T, \epsilon, \tau). \quad (2.35)$$

$$\begin{aligned} \tilde{f}_\Gamma(x, b_\perp, P^z; \mu) &= H_f(x, P^z; \mu) B(x, b_\perp, xP^+; \mu, \nu) \\ &\times S_C^0(b_\perp; \mu, \nu), \end{aligned} \quad (3)$$

$$\begin{aligned} \sqrt{S_I(b_\perp, y_n; \mu)} \cdot \tilde{f}_\Gamma(x, b_\perp, P^z; \mu) \\ = f(x, b_\perp; \mu, \zeta) H_f(x, P^z; \mu) + \text{p.c.}, \end{aligned} \quad (5)$$

- Zero-bin subtracted beam function has no soft contribution;
- S_C^0 is the quasi-soft function with zero-bin contribution;
- The intrinsic soft function S_I is the combination of subtracted soft function and the quasi-soft function



Fermilab

Fermi *FORWARD*



U.S. DEPARTMENT
of ENERGY